POLITECNICO DI TORINO
Repository ISTITUZIONALE

A Yukawa-Calderón Time-Domain Combined Field Integral Equation for Electromagnetic Scattering

Original
A Yukawa-Calderón Time-Domain Combined Field Integral Equation for Electromagnetic Scattering / Le, V.C., Cordel, P., Andriulli, F.P., Cools, K.. - ELETTRONICO. - (2023), pp. 292-295. (24th International Conference on Electromagnetics in Advanced Applications (ICEAA) Venice (Italy) 09-13 October 2023) [10.1109/iceaa57318.2023.10297732].

Availability:
This version is available at: 11583/2992544 since: 2024-10-14T15:46:16Z

Publisher:
IEEE

Published
DOI:10.1109/iceaa57318.2023.10297732

Terms of use:

This article is made available under terms and conditions as specified in the corresponding bibliographic description in the repository

Publisher copyright
IEEE postprint/Author's Accepted Manuscript

©2023 IEEE. Personal use of this material is permitted. Permission from IEEE must be obtained for all other uses, in any current or future media, including reprinting/republishing this material for advertising or promotional purposes, creating new collecting works, for resale or lists, or reuse of any copyrighted component of this work in other works.

(Article begins on next page)

10 October 2026

A Yukawa-Calderón Time-Domain Combined Field Integral Equation for Electromagnetic Scattering

Van Chien Le*, Pierrick Cordel†, Francesco P. Andriulli†, Kristof Cools*
*IDLab, Department of Information Technology, Ghent University - imec, 9000 Ghent, Belgium
Email: vanchien.le@ugent.be; kristof.cools@ugent.be
†Department of Electronics and Telecommunications, Politecnico di Torino, 10129 Turin, Italy
Email: pierrick.cordel@polito.it; francesco.andriulli@polito.it

***Abstract*—This paper introduces a Yukawa-Calderón time-domain combined field integral equation for electromagnetic scattering by a perfect electric conductor. The time-domain electric and magnetic field integral operators are composed with Yukawa-type integral operators. The linearly combined formulation is well-conditioned when the spatial discretization is dense, and it is also free from interior resonant frequencies. Several numerical results corroborate the properties of the proposed formulation.**

***Index Terms*—TD-CFIE, Marching-on-in-time, Yukawa-type integral operators, Calderón preconditioning**

I. Introduction

Analyzing transient electromagnetic scattering by perfect electric conductors (PECs) primarily uses the time-domain electric field integral equation (TD-EFIE) and the time-domain magnetic field integral equation (TD-MFIE). Besides many advantages, marching-on-in-time (MOT) boundary element formulations of the TD-EFIE and TD-MFIE suffer from some numerical issues, including dense discretization breakdown and resonant instability. The Calderón preconditioning has been known as a common strategy to prevent EFIE systems from being ill-conditioned when the spatial discretization is dense [1]. The instability caused by resonant frequencies of PEC can be overcome using time-domain combined field integral equations (TD-CFIEs) [2]. An appropriate Calderón preconditioned TD-CFIE, therefore, can combat both dense discretization breakdown and resonant instability, see, e.g., [3].

In this contribution, we propose a TD-CFIE formulation which is immune to both dense discretization breakdown and resonant instability. The TD-EFIE and TD-MFIE operators are respectively composed with the Yukawa-type EFIE and MFIE operators. The proposed formulation is discretized using a space-time Galerkin discretization scheme, and the resulting matrix system is solved using the MOT algorithm. Several numerical experiments performed for different geometries corroborate the properties of the Yukawa-Calderón TD-CFIE.

The novelty of this work lies in the introduction of a symmetrized MFIE operator. The goal of introducing this operator is to render the proposed TD-CFIE stable at large-time steps by a discrete Helmholtz decomposition. However, this stabilization falls within the scope of another work.

V. C. Le and K. Cools were supported by the European Research Council through the European Union's Horizon 2020 Research and Innovation programme (Grant number 101001847).

II. Formulation

A. Time-domain boundary integral equations

Let Ω be a PEC in $\mathbb{R}^3$ with a closed boundary Γ. We denote by $\mathbf{n}$ the outward normal vector on Γ. An incident electromagnetic wave $(\boldsymbol{e}^{in}, \boldsymbol{h}^{in})$ induces a surface current $\boldsymbol{j}$ on Γ, which satisfies the following TD-EFIE and TD-MFIE

$$(\mathcal{T}\boldsymbol{j})(\boldsymbol{r},t) = -\mathbf{n}\times\boldsymbol{e}^{in}(\boldsymbol{r},t), \tag{1}$$

$$\left(\frac{1}{2}\mathcal{I}+\mathcal{K}\right)\boldsymbol{j}(\boldsymbol{r},t) = \mathbf{n}\times\boldsymbol{h}^{in}(\boldsymbol{r},t), \tag{2}$$

for all $\boldsymbol{r}\in\Gamma$ and $t>0$. Here, $\mathcal{I}$ is the identity operator, and the time-domain integral operators $\mathcal{T}$ and $\mathcal{K}$ are defined as

$$(\mathcal{T}\boldsymbol{j})(\boldsymbol{r},t) = \frac{\eta}{c}(\mathcal{T}^s\boldsymbol{j})(\boldsymbol{r},t) + c\eta\,(\mathcal{T}^h\boldsymbol{j})(\boldsymbol{r},t),$$

$$(\mathcal{T}^s\boldsymbol{j})(\boldsymbol{r},t) = -\mathbf{n}\times\int_\Gamma \frac{\partial_t\boldsymbol{j}(\boldsymbol{r}',\tau)}{4\pi R}\,\mathrm{d}s',$$

$$(\mathcal{T}^h\boldsymbol{j})(\boldsymbol{r},t') = \mathbf{n}\times\mathbf{grad}_{\mathbf{x}}\int_{-\infty}^{t'}\int_\Gamma \frac{\mathrm{div}_\Gamma\,\boldsymbol{j}(\boldsymbol{r}',\tau)}{4\pi R}\,\mathrm{d}s'\,\mathrm{d}t,$$

$$(\mathcal{K}\boldsymbol{j})(\boldsymbol{r},t) = -\mathbf{n}\times\mathbf{curl}_{\mathbf{x}}\int_\Gamma \frac{\boldsymbol{j}(\boldsymbol{r},\tau)}{4\pi R}\,\mathrm{d}s',$$

where $\eta=\sqrt{\mu/\epsilon}$ is the impedance, $c=1/\sqrt{\mu\epsilon}$ is the speed of light, ϵ and μ are the permittivity and permeability of vacuum. Moreover, $R=|\boldsymbol{r}-\boldsymbol{r}'|$ and $\tau=t-R/c$.

B. Yukawa-type integral operators

In order to avoid composition EFIE and MFIE operators sharing their common resonant frequencies, we introduce the following integral operators for the Yukawa-type equation

$$(T_{-j\kappa}\boldsymbol{j})(\boldsymbol{r}) = \eta\kappa\,(T^s_{-j\kappa}\boldsymbol{j})(\boldsymbol{r}) + \frac{\eta}{\kappa}(T^h_{-j\kappa}\boldsymbol{j})(\boldsymbol{r}),$$

$$(T^s_{-j\kappa}\boldsymbol{j})(\boldsymbol{r}) = \mathbf{n}\times\int_\Gamma \frac{e^{-\kappa R}}{4\pi R}\,\boldsymbol{j}(\boldsymbol{r}')\,\mathrm{d}s',$$

$$(T^h_{-j\kappa}\boldsymbol{j})(\boldsymbol{r}) = -\mathbf{n}\times\mathbf{grad}_{\mathbf{x}}\int_\Gamma \frac{e^{-\kappa R}}{4\pi R}\,\mathrm{div}_\Gamma\,\boldsymbol{j}(\boldsymbol{r}')\,\mathrm{d}s',$$

$$(K_{-j\kappa}\boldsymbol{j})(\boldsymbol{r}) = -\mathbf{n}\times\mathbf{curl}_{\mathbf{x}}\int_\Gamma \frac{e^{-\kappa R}}{4\pi R}\,\boldsymbol{j}(\boldsymbol{r}')\,\mathrm{d}s',$$

with a fixed $\kappa>0$. The operators $T_{-j\kappa}$ and $K_{-j\kappa}$ are respectively identical with the frequency-domain (FD) EFIE and MFIE operators with imaginary wave number $-j\kappa$.

C. Yukawa-Calderón TD-CFIE

The idea of considering a Yukawa-Calderón TD-CFIE comes from the Yukawa-Calderón FD-CFIE proposed in [4], which is defined for the wave number κ as follows

$$\begin{aligned}&\left(-T_{-j\kappa}T_\kappa+\alpha\left(\frac{1}{2}I-K_{-j\kappa}\right)\left(\frac{1}{2}I+K_\kappa\right)\right)\boldsymbol{j}(r)\\&=T_{-j\kappa}\left(\mathbf{n}\times\boldsymbol{e}^{in}(\boldsymbol{r})\right)+\alpha\left(\frac{1}{2}I-K_{-j\kappa}\right)\left(\mathbf{n}\times\boldsymbol{h}^{in}(\boldsymbol{r})\right),\end{aligned}\tag{3}$$

with a coefficient $\alpha>0$. The operator $T_{-j\kappa}$ plays the role of a preconditioner to T_κ. The FD-CFIE formulation (3) is well-conditioned and invertible for any $\kappa>0$. Moreover, when replacing the operators T_κ and K_κ respectively by $T_{\kappa'}$ and $K_{\kappa'}$ with $\kappa'\neq\kappa$ (meanwhile fixing $T_{-j\kappa}$ and $K_{-j\kappa}$), we notice that the resulting equation stays well-conditioned and resonant-free. Its inverse Fourier transform with respect to κ' gives rise to the following Yukawa-Calderón TD-CFIE

$$\begin{aligned}&\left(-T_{-j\kappa}\mathcal{T}+\alpha\left(\frac{1}{2}I-K_{-j\kappa}\right)\left(\frac{1}{2}\mathcal{I}+\mathcal{K}\right)\right)\boldsymbol{j}(\boldsymbol{r},t)\\&=T_{-j\kappa}\left(\mathbf{n}\times\boldsymbol{e}^{in}(\boldsymbol{r},t)\right)+\alpha\left(\frac{1}{2}I-K_{-j\kappa}\right)\left(\mathbf{n}\times\boldsymbol{h}^{in}(\boldsymbol{r},t)\right).\end{aligned}\tag{4}$$

III. Discretization

In order to numerically solve (4) using the boundary element method, the surface Γ is partitioned into triangles with N_S edges. The Yukawa-type EFIE operator $T_{-j\kappa}$ is discretized using Buffa-Christiansen (BC) functions $\boldsymbol{g}_m$. The operators I and $K_{-j\kappa}$ are expanded by Rao-Wilton-Glisson (RWG) functions $\boldsymbol{f}_m$, and tested with rotated BC functions $\mathbf{n}\times\boldsymbol{g}_m$. More specifically, we define the following matrices

$$\begin{aligned}[\mathbb{G}]_{mn}&=\langle\mathbf{n}\times\boldsymbol{g}_m,\boldsymbol{f}_n\rangle,\\[\mathbb{Z}]_{mn}&=\langle\mathbf{n}\times\boldsymbol{g}_m,T_{-j\kappa}\boldsymbol{g}_n\rangle,\\[\mathbb{M}]_{mn}&=\langle\mathbf{n}\times\boldsymbol{g}_m,K_{-j\kappa}\boldsymbol{f}_n\rangle,\end{aligned}$$

where

$$\langle\boldsymbol{f},\boldsymbol{g}\rangle=\int_\Gamma\boldsymbol{f}(\boldsymbol{r})\cdot\boldsymbol{g}(\boldsymbol{r})\,\mathrm{d}s.$$

The unknown current density $\boldsymbol{j}(\boldsymbol{r},t)$ is approximated as an expansion in the set of N_S spatial RWG basis functions $\boldsymbol{f}_m(\boldsymbol{r})$ and N_T temporal basis functions $h_i(t)$ as follows

$$\boldsymbol{j}(\boldsymbol{r},t)\approx\sum_{m=1}^{N_S}\sum_{i=1}^{N_T}[\mathrm{j}_i]_m\,\boldsymbol{f}_m(\boldsymbol{r})h_i(t).\tag{5}$$

Here, the shifted temporal functions $h_i(t)=h_0(t-i\Delta t)$, with $i=1,2,\ldots,N_T$, and the function h_0 is defined by

$$h_0(t)=\begin{cases}1+\frac{t}{\Delta t} & \text{if } -\Delta t<t<0,\\ 1-\frac{t}{\Delta t} & \text{if } 0\le t<\Delta t,\\ 0 & \text{otherwise,}\end{cases}$$

where Δt is the time step (see Fig. 1).

The TD-EFIE (1) is spatially tested with rotated RWG functions $\mathbf{n}\times\boldsymbol{f}_m$ and then evaluated at each time step $t=k\Delta t$

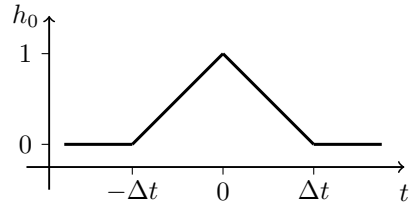

Fig. 1. The temporal basis function h_0.

with $k=1,2,\ldots,N_T$, resulting in the following block matrix equation

$$\begin{pmatrix}\mathbf{Z}_0 & & & \\ \mathbf{Z}_1 & \mathbf{Z}_0 & & \\ \vdots & \vdots & \ddots & \\ \mathbf{Z}_{N_T-1} & \mathbf{Z}_{N_T-2} & \cdots & \mathbf{Z}_0\end{pmatrix}\begin{pmatrix}\mathrm{j}_1\\ \mathrm{j}_2\\ \vdots\\ \mathrm{j}_{N_T}\end{pmatrix}=\begin{pmatrix}\mathrm{e}_1\\ \mathrm{e}_2\\ \vdots\\ \mathrm{e}_{N_T}\end{pmatrix},$$

or equivalently

$$\mathbf{Z}\,\mathrm{j}=\mathrm{e}.\tag{6}$$

Similarly, the TD-MFIE (2) is spatially tested with rotated BC functions $\mathbf{n}\times\boldsymbol{g}_m$, which results in

$$\left(\frac{1}{2}\,\mathbf{G}+\mathbf{M}\right)\mathrm{j}=\mathrm{h}.\tag{7}$$

The block matrices in (6) and (7) are defined by

$$\begin{aligned}[\mathrm{e}_i]_m&=\left\langle\mathbf{n}\times\boldsymbol{f}_m,\mathbf{n}\times\boldsymbol{e}^{in}\right\rangle\big|_{t=i\Delta t},\\[\mathrm{h}_i]_m&=\left\langle\mathbf{n}\times\boldsymbol{g}_m,\mathbf{n}\times\boldsymbol{h}^{in}\right\rangle\big|_{t=i\Delta t},\\[\mathbf{Z}_i]_{mn}&=\langle\mathbf{n}\times\boldsymbol{f}_m,\mathcal{T}\left(\boldsymbol{f}_n h_i\right)\rangle|_{t=0},\\[\mathbf{M}_i]_{mn}&=\langle\mathbf{n}\times\boldsymbol{g}_m,\mathcal{K}\left(\boldsymbol{f}_n h_i\right)\rangle|_{t=0}.\end{aligned}$$

Moreover, $\mathbf{G}_0=\mathbb{G}$ and $\mathbf{G}_i=0$ for $i\neq0$. To conclude, we solve the following discretized matrix system of the Yukawa-Calderón TD-CFIE (4)

$$\mathbf{L}\,\mathrm{j}=\mathrm{r},\tag{8}$$

where the right-hand side

$$\mathrm{r}_i:=-\mathbb{Z}\mathbb{G}^{-\mathsf{T}}\mathrm{e}_i+\alpha\left(\frac{1}{2}\mathbb{G}-\mathbb{M}\right)\mathbb{G}^{-1}\mathrm{h}_i,$$

and the left-hand side

$$\mathbf{L}_i:=\mathbb{Z}\mathbb{G}^{-\mathsf{T}}\,\mathbf{Z}_i+\alpha\left(\frac{1}{2}\mathbb{G}-\mathbb{M}\right)\mathbb{G}^{-1}\left(\frac{1}{2}\,\mathbf{G}_i+\mathbf{M}_i\right).$$

Please note that the inverse Gram matrices $\mathbb{G}^{-\mathsf{T}}$ and $\mathbb{G}^{-1}$ are inserted to ensure the compatibility of the discretization of composition operators. Equation (8) can be efficiently solved using the MOT algorithm

$$\mathrm{j}_k=\mathbf{L}_0^{-1}\left(\mathrm{r}_k-\sum_{i=1}^{k-1}\mathbf{L}_i\,\mathrm{j}_{k-i}\right).$$

Remark 3.1: There is no specific rule for the choice of κ. However, we would recommend to choose κ of the order of $(c\Delta t)^{-1}$ to preserve the behavior of time-domain operators.

IV. Numerical results

In this section, several numerical experiments are performed for different geometries (see Fig. 2):

A. a sphere (smooth and simply-connected),
B. a cuboid (non-smooth and simply-connected),
C. a torus (smooth and multiply-connected).

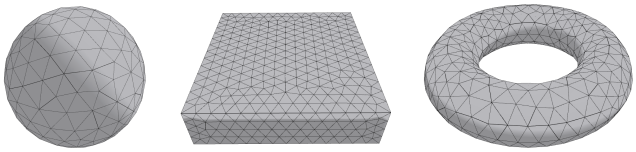

Fig. 2. Triangle mesh of different geometries used in numerical experiments. *Left:* a sphere with radius 1m discretized by 476 triangles. *Middle:* a cuboid of dimensions $0.5\text{m} \times 2\text{m} \times 2\text{m}$ discretized by 1428 triangles. *Right:* a torus with two radii 3m and 1m discretized into 952 triangles.

These PEC bodies are illuminated by a Gaussian-in-time plane wave

$$\boldsymbol{e}^i(\boldsymbol{r},t) = \frac{4A}{w\sqrt{\pi}}\boldsymbol{p}\exp\left(-\left(\frac{4}{w}\left(c(t-t_0)-\boldsymbol{k}\cdot\boldsymbol{r}\right)\right)^2\right),$$

with amplitude $A = 1\text{V}$, width $w = 26.67\text{m}$, polarization $\boldsymbol{p} = \mathbf{1}_x$, direction $\boldsymbol{k} = \mathbf{1}_z$, and time of arrival $t_0 = 80\text{ns}$. The time step $\Delta t = 0.333\text{ns}$. Numerical results are obtained using different formulations:

- the standard TD-EFIE (6);
- the standard TD-MFIE (7);
- the mixed TD-CFIE proposed in [2] with $\alpha = 0.5$;
- the proposed Yukawa-Calderón (YC) TD-CFIE (8) with coefficients $\alpha = \eta^2$ and $\kappa = (c\Delta t)^{-1}$.

A. Scattering by a sphere

We firstly examine scattering by a PEC sphere with radius 1m, which is approximated by 476 triangles (Fig. 2, left). The unknown current density $\boldsymbol{j}$ is computed via expansion coefficients of 714 spatial RWG basis functions and 1200 temporal basis functions. The current density intensities at the point $(x, y, z) = (-0.534, -0.523, -0.644)\text{m}$ on the sphere are shown in Fig. 3. At early times ($t < 150\text{ns}$), four formulations give identical results. After that, however, the impact of resonant frequencies on the TD-EFIE and TD-MFIE becomes significant, preventing their solutions from decaying. On the other hand, the mixed TD-CFIE and the Yukawa-Calderón TD-CFIE do not suffer from resonant instability. They match well up to the finite numerical precision.

The condition number of the matrix $\mathbf{L}_0$ with respect to different mesh sizes h are presented in Fig. 4. The condition numbers of the TD-EFIE and the mixed TD-CFIE respectively grow with orders $\mathcal{O}(h^{-2})$ and $\mathcal{O}(h^{-1})$, whereas the condition numbers of the TD-MFIE and the Yukawa-Calderón TD-CFIE stay constants. This shows that the proposed TD-CFIE (4) is well-conditioned when the spatial discretization is dense.

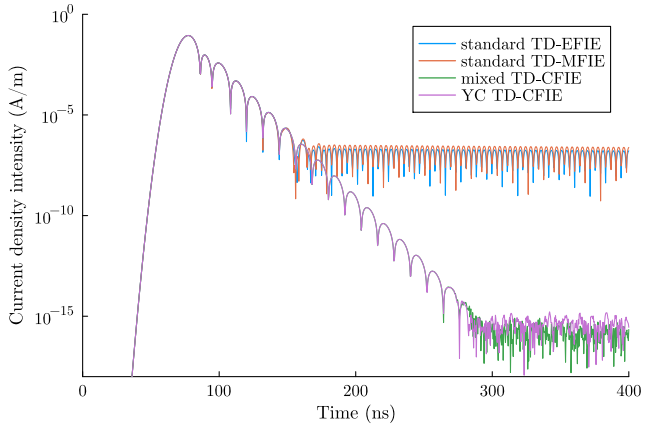

Fig. 3. Induced surface current density intensity on a sphere of radius 1m at the point $(x, y, z) = (-0.534, -0.523, -0.644)\text{m}$, obtained using different formulations. The average mesh size $h = 0.3\text{m}$, and the time step $\Delta t = 0.333\text{ns}$. The TD-EFIE and TD-MFIE suffer from resonant instability, whereas the TD-CFIEs do not.

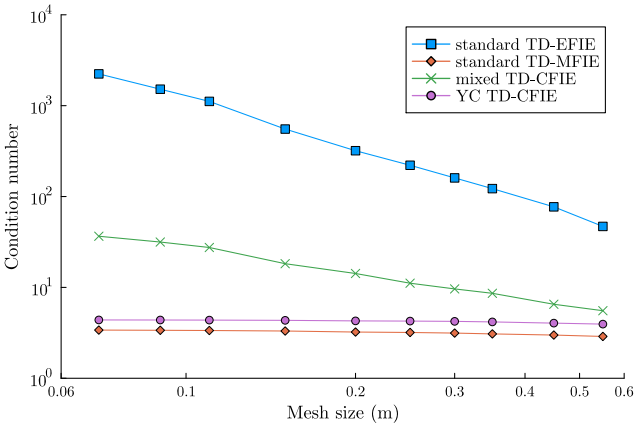

Fig. 4. Condition number of the matrix $\mathbf{L}_0$ with respect to different mesh sizes of a sphere with radius 1m, obtained using different formulations. The time step is fixed at $\Delta t = 3.33\text{ns}$. The TD-MFIE and the Yukawa-Calderón TD-CFIE stay well-conditioned when the mesh size decreases.

B. Scattering by a cuboid

We consider a PEC cuboid of dimensions $0.5\text{m} \times 2\text{m} \times 2\text{m}$ which is partitioned into 1428 triangles (Fig. 2, middle). The induced current density $\boldsymbol{j}$ is expanded by 2142 spatial RWG basis functions and 1200 temporal basis functions. Since the domain is non-smooth, the simulations require interaction integrals must be computed with higher accuracy to retain the same level of solution errors as for smooth domains. The solutions to different formulations are depicted in Fig. 5. Four formulations match very well until $t = 110\text{ns}$. The standard TD-EFIE and TD-MFIE suffer from resonant instability, whereas the induced currents obtained using the mixed TD-CFIE and the Yukawa-Calderón TD-CFIE decay to the machine precision. The condition numbers of different formulations for the cuboid are shown in Fig. 6, which confirms the well-conditionedness of the proposed TD-CFIE when the mesh size decreases.

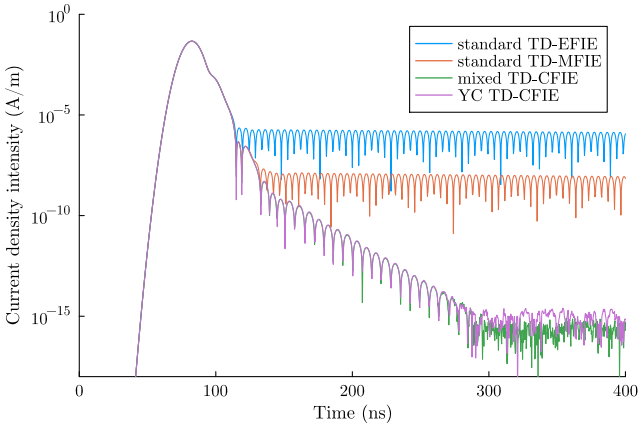

Fig. 5. Induced surface current density intensity on a cuboid of dimensions $0.5\text{m}\times2\text{m}\times2\text{m}$ at the point $(x, y, z) = (-0.25, -0.502, 0.761)\text{m}$, obtained using different formulations. The average mesh size $h = 0.15\text{m}$, and the time step $\Delta t = 0.333\text{ns}$. The TD-EFIE and TD-MFIE suffer from resonant instability, whereas the TD-CFIEs do not.

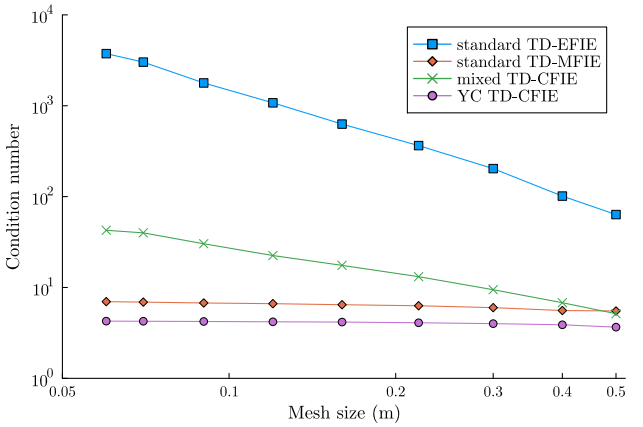

Fig. 6. Condition number of the matrix $\mathbf{L}_0$ with respect to different mesh sizes of a cuboid of dimensions $0.5\text{m} \times 2\text{m} \times 2\text{m}$, obtained using different formulations. The time step is fixed at $\Delta t = 3.33\text{ns}$. The TD-EFIE and the mixed TD-CFIE exhibit dense discretization breakdown, whereas the TD-MFIE and the Yukawa-Calderón TD-CFIE do not.

C. Scattering by a torus

Scattering by a PEC torus with large radius 3m and small radius 1m (Fig. 2, right) is now studied. The time evolution of the induced current density $\boldsymbol{j}$ obtained using different formulations are illustrated in Fig. 7. The oscillating non-decaying mode is observed in the tail of TD-EFIE's and TD-MFIE's solutions, which can be interpreted as the effect of resonant frequencies of the interior domain. As the surface is toroidal (multiply-connected), the TD-MFIE is also notorious for being affected by the nontrivial nullspace of the static MFIE operator [5]. This can be corroborated by the oscillation of the amplitude of the TD-MFIE solution. The TD-CFIEs both are resonant-free, but their solutions are slowly decaying. The condition numbers of different formulations for the torus are depicted in Fig. 8. This figure convinces us again that the proposed Yukawa-Calderón TD-CFIE does not suffer from dense discretization breakdown.

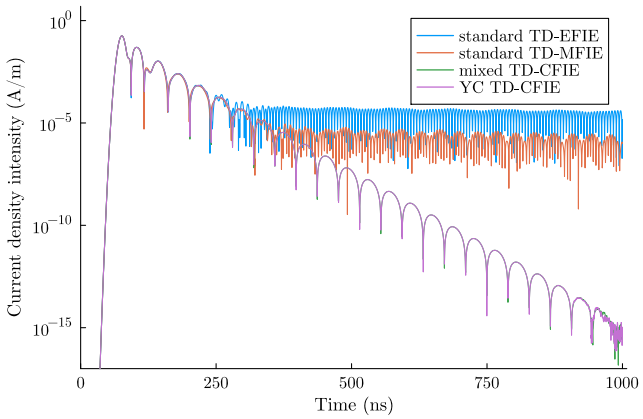

Fig. 7. Induced surface current density on a torus with two radii 3m and 1m at the point $(x, y, z) = (-2.326, -1.885, -0.692)\text{m}$, obtained using different formulations. The average mesh size $h = 0.6\text{m}$, and the time step $\Delta t = 0.333\text{ns}$. The TD-EFIE and TD-MFIE suffer from resonant instability. The TD-MFIE is also affected by the nontrivial nullspace of the static MFIE operator. The TD-CFIEs are resonant-free, but slowly decay.

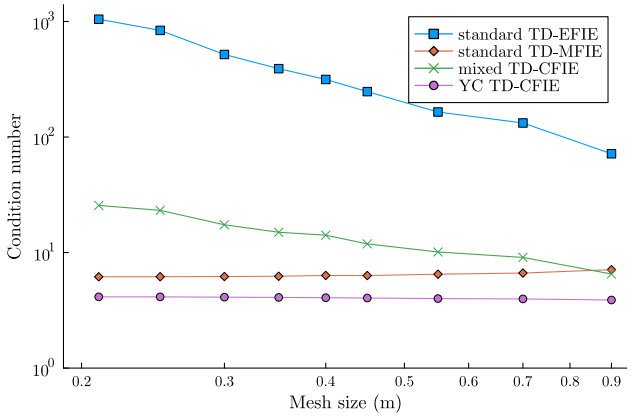

Fig. 8. Condition number of the matrix $\mathbf{L}_0$ with respect to different mesh sizes of a torus with large radius 3m and small radius 1m, obtained using different formulations. The time step is fixed at $\Delta t = 6.67\text{ns}$. The TD-MFIE and the Yukawa-Calderón TD-CFIE do not suffer from dense discretization breakdown.

References

[1] K. Cools, F. P. Andriulli, F. Olyslager, and E. Michielssen, "Time domain Calderón identities and their application to the integral equation analysis of scattering by PEC objects Part I: Preconditioning," *IEEE Trans. Antennas Propag.*, vol. 57, no. 8, pp. 2352–2364, 2009.

[2] Y. Beghein, K. Cools, H. Bagci, and D. De Zutter, "A space-time mixed Galerkin marching-on-in-time scheme for the time-domain combined field integral equation," *IEEE Trans. Antennas Propag.*, vol. 61, no. 3, pp. 1228–1238, 2013.

[3] F. P. Andriulli, K. Cools, F. Olyslager, and E. Michielssen, "Time domain Calderón identities and their application to the integral equation analysis of scattering by PEC objects Part II: Stability," *IEEE Trans. Antennas Propag.*, vol. 57, no. 8, pp. 2365–2375, 2009.

[4] A. Merlini, Y. Beghein, K. Cools, E. Michielssen, and F. P. Andriulli, "Magnetic and combined field integral equations based on the quasi-Helmholtz projectors," *IEEE Trans. Antennas Propag.*, vol. 68, no. 5, pp. 3834–3846, 2020.

[5] K. Cools, F. P. Andriulli, F. Olyslager, and E. Michielssen, "Nullspaces of MFIE and Calderón preconditioned EFIE operators applied to toroidal surfaces," *IEEE Trans. Antennas Propag.*, vol. 57, no. 10, pp. 3205–3215, 2009.